Journal of Materials Science: Materials in Medicine (2024) 35:72
https://doi.org/10.1007/s10856-024-06812-z

BIOMATERIALS SYNTHESIS AND CHARACTERIZATION

Original Research

Synthesis, characterization, and application potential of chitosan/acrylamide composite hydrogels as skin expanders

Chenxi Zhang[1] · Chenjie Tan[2] · Hangchong Shen[1] · Qianqian Xu[1] · Jiadong Pan[1] · Xin Wang[1]

Received: 17 November 2023 / Accepted: 2 July 2024 / Published online: 30 November 2024

Abstract

Hydrogels are currently widely used in regenerative medicine and wound repair due to their superior biocompatibility, reliable mechanical strength, and good morphological memory. We aimed to prepare a self-expanding hydrogel that can be used as a skin expander for the repair of large soft skin tissue defects. Self-expanding hydrogels were prepared by chemical cross-linking, which consisted of water-soluble chitosan (CS), acrylamide (AM), methylene bisacrylamide (NMBA), etc. Five groups of in vitro experiments, including (CS-AM) of 0% (pure AM group), 13.9%, 27.8%, 41.7%, and 55.6%, were conducted to determine mechanical properties, swelling properties, cytotoxicity, etc. In the rat model, both a tight skin area (neck) and a loose skin area (back) were selected for expansion with hydrogels. A total of 27.8% of the CS-AM samples expanded stably under the skin of the rats, achieving 370% expansion in the tight zone and 490% expansion in the flaccid zone. Subcutaneous histopathological examination suggested that the inflammation index of the pericolloid tissue was lower in the CS-AM group than in the pure AM group. Our results demonstrate that self-expanding CS-AM hydrogels have great potential for application as skin expanders.

Graphical Abstract

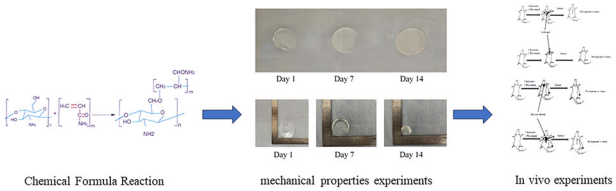

1 Introduction

Large skin defects caused by severe trauma, burns, and large tumor removal cause severe physical and psychological trauma to patients but are still clinically difficult to repair, most importantly due to the lack of suitable local tissue coverage [1, 2]. Neumann pioneered soft tissue skin expansion in 1957 when he used a polyethylene balloon to inflate and expand the skin of the ear to repair a partial ear defect after trauma [3]. In recent years, a large number of scholars have conducted extensive and systematic research on tissue expansion techniques involving clinical and basic theory and have accumulated extensive experience [4]. However, currently, the treatment period is long, with patients generally requiring 3 to 4 months of treatment [5]. The advent of skin dilators has provided a new means of solving this problem. The advent of skin and soft tissue

These authors contributed equally: Chenxi Zhang, Chenjie Tan, Jiadong Pan, Xin Wang

✉ Jiadong Pan
emilon@sina.com

✉ Xin Wang
drwangxinnb@126.com

[1] Department of Plastic Reconstructive Surgery & Hand Microsurgery, Ningbo NO.6 Hospital, 1059 East Zhongshan Road, Ningbo, China

[2] Department of Orthopedics, Huzhou Central Hospital, Huzhou Basic and Clinical Translation of Orthopedics Key Laboratory, Huzhou, Zhejiang, PR China

dilators is a milestone in the plastic surgery field [6]. Most tissue expanders are silicone elastomer balloons that are surgically placed under the skin and expand over the course of a few weeks [7]. However, this method often leads to complications such as hematomas, wound infections, and reservoir balloon rupturing [8, 9].

Self-expanding hydrogels are novel expanders that have been used for the treatment of anophthalmia, cryptophthalmia, and scarring in children and are superior to conventional expanders in terms of postoperative complications [10, 11]. It should be noted, however, that self-expanding hydrogels absorb tissue fluid autonomously for expansion, and their rate of expansion is not easy to control, which is a key problem that has prevented the widespread use of hydrogel dilators. The second generation of self-swelling hydrogel expanders has been improved based on the first generation by adding aa plastic shell to decrease the unopposed expansion that occurred in first-generation expanders, which led to pressure necrosis of the skin flaps [5]. However, second-generation self-expanding hydrogels can only be used in loose and small areas, while large wound defects require a greater amount of soft tissue [12, 13]. In addition, most hydrogels lack the required mechanical properties [14]. The low mechanical strength cannot withstand the deformation caused by expansion, which severely limits the use of skin extenders. Finally, the ability of the hydrogel skin expander to moisturize is also critical [15]. Therefore, the ideal hydrogel skin expander should have the following characteristics: good mechanical properties, swelling properties, and moisturizing properties [16, 17]. We aim to create a hydrogel extender that can be swelled by water or tissue fluid within a short time and maintain good stability and structural strength throughout the swelling process while ensuring that the effect of the hydrogel on surrounding soft tissues is safe and controllable. In addition, according to the skin creep characteristics, the expansion of the skin surface area by the hydrogel should be controlled to approximately 4 times, and the total swelling time should be controlled at 2–3 weeks, which would meet the urgent need for this type of expander in clinical practice.

AM is a man-made organic compound with an amide group and carbon–carbon double bond that readily polymerizes [18]. Acrylamide hydrogels have strong degradation resistance and shear resistance, but hydrogels made from only AM are poorly shaped and have deficiencies in tensile properties, light transmission, long-term stability, and environmental sensitivity, making them difficult to use in clinical applications [19]. In this study, AM was polymerized with another polymeric colloidal network (chitosan), and it was demonstrated through experimental tests that this method enhanced the gel mechanics, histocompatibility, and swelling properties of the material compared with pure AM, suggesting that this material has the potential to be developed as a new soft tissue expander. As a biodegradable polymer with excellent properties, chitosan is widely used in medical materials [20]. In addition, chitosan has been shown to have good swelling capacity, mechanical strength, and antibacterial properties [21–23]. Chitosan is one of the most widely used materials in the manufacture of hydrogels.

Herein, for the first time, we report a self-expanding hydrogel skin extender with good mechanical properties, reliable swelling properties, and *moisturizing* properties and explore its beneficial properties in a rat model.

2 Materials and methods

2.1 Experimental reagents

The main materials used were as follows: water-soluble chitosan (chitosan, CS) from Shandong HeKou Wang Biotechnology Co., Ltd.; acrylamide (AM) from Lushi Guoyao Group; N,N-methylene bisacrylamide from Aegis Chemical, Sarn Chemical Technology (Shanghai) Co. Maclean's Biochemical Technology Co., Ltd.; ethylene glycol from Lushi Guoyao Group; and a silicone dilator from YuYao Jiu Sheng Medical Supplies Co.

The main instruments used were an HJ-6B double digital display multistation magnetic stirrer from Xinbao Instrument Company; an ultrasonic oscillator from Shenzhen Guanboshi Company; a vacuum drying oven from Shanghai Hengyi Company; a rubber mold from Rongtai Plastic Industry Co., Ltd.; a horizontal rotator from Jiangsu Tianling Instrument Co., Ltd.; a Scientz2 5 T vacuum lyophilizer from Ningbo Xinzhi Biotechnology Co., Ltd.; an FEI Quanta 450 field emission scanning electron microscope, Ltd.; an FEI Quanta 450 Field Emission Scanning Electron Microscope, USA; and an Edberg HLD Digital Push-Pull Meter from Yueqing Edberg Instruments Co.

2.2 Preparation of self-expanding hydrogels

First, 0.5 g, 1.0 g, 1.5 g, and 2.0 g of CS were added to beakers containing 20 ml of deionized water. The above four groups were designated the experimental groups, and a control group (pure AM group) without the enhancing agent CS was designed using 20 ml of deionized water as the solvent. The experimental groups were subjected to the following steps: (1) each group was heated to approximately 45 °C with a constant-temperature magnetic stirrer and stirred until complete swelling of the CS was achieved, after which the reaction was continued for 1 h; the pure AM group was allowed to stand at room temperature for 10 min. (2) The solution temperature of each group (including the

pure AM group) was maintained at 50 °C, 3.6 g of AM was added to each group, the mixture was stirred until complete swelling was achieved, and the reaction was continued for 30 min. (3) First, 1.2 ml of the prepared N,N-methylene bisacrylamide solution (NMBA, 1 g/L) was added to the solution and allowed to react for 10 min. (4) Then, 0.4 g of potassium persulfate (KBS) was added, and the mixture was stirred for 10 min. (5) After each group of solutions was clarified, the liquid was poured into a circular rubber orifice plate with a diameter of 3 cm and a height of 2 cm. (6) The orifice plate containing the solution was placed in an ultrasonic cleaning machine for degassing for 30 min, and then it was heated to 60 °C using the cleaning machine. At this temperature, the solution was fixed at a constant temperature, and this process took approximately 1 h. (7) The formed hydrogel sample was placed in a beaker containing deionized water. The beaker was placed on a horizontal rotator. The horizontal rotator rotated at a speed of 80 rpm. The gel was washed with deionized water. The deionized water was replaced once an hour three times. (8) After washing, the colloid was soaked in a 1 mol/L calcium chloride solution for 1 h. (9) After soaking, the colloid was washed with a 1 mol/L NaOH solution for 1 h, as described above. 10) The colloid was soaked in ethylene glycol solution and replaced every hour for a total of 3 times. 11) Finally, a large amount of deionized water was used to clean the colloid, and the finished colloid was placed in a vacuum drying box and stored at 25 °C for future use. (12) According to the mass ratio of CS to AM during the preparation of colloids, the final gels were named the CS-AM 13.9%, CS-AM 27.8%, CS-AM 41.7%, CS-AM 55.6%, and pure AM (0%) groups. In the thermal reaction process, the unsaturated carbon–carbon double bond and amide bond of AM are recrosslinked due to the addition of CS (Fig. 1).

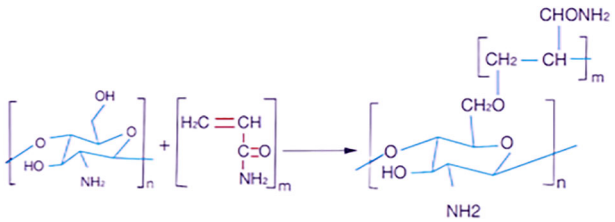

Fig. 1 Chemical formula reaction of chitosan and polyacrylamide

2.3 Hydrogel mechanical property experiments

(1) Compression strength test

The prepared hydrogels ($n = 4$) were cut into cylindrical samples 1 cm in height and 3 cm in diameter at room temperature. Compression testing of the hydrogel was conducted with a digital display push-pull meter, and the compression endpoint was when the gel ruptured or the compression rate reached 100% (the compression sheets adhered to each other), and the compression rate was set to 0.05 cm/s. The average value of four experiments was taken, and finally, the compression performance curve was plotted.

(2) Tensile test

For the tensile experiment, the hydrogels ($n = 4$) were prepared to a size of 2 × 0.5 × 0.5 cm, placed on a push-pull meter with the upper and lower ends fixed, and stretched at a constant speed of 0.2 cm/s (Fig. 2). The value (N) at the time of pull-off or maximum tension was recorded, and the final tensile rate (%) was calculated. The tensile rate formula is tensile rate = L1/L0*100%, where L1 is the length of the gel at break and L0 is the initial length. Four measurements were taken for each gel, the final average was taken, and finally, the tensile performance curve was plotted.

2.4 Hydrogel in vitro swelling experiments

Four hydrogels were prepared and randomly numbered for the swelling test. The initial volume of the finished colloid was measured with a 3D laser scanner and recorded as V0. The different colloids were placed in separate beakers, and the PBS buffer was added until the colloid was completely

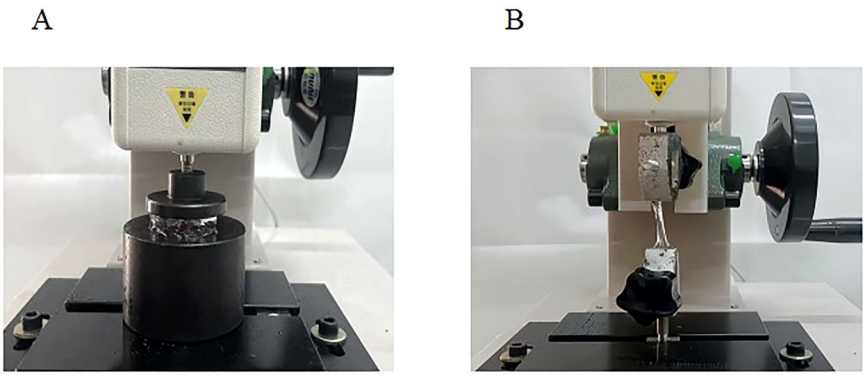

Fig. 2 **A** Compression of the hydrogel; **B** Stretching of the hydrogel

submerged [24]. The containers were placed in a thermostat set at 37 °C. The gel was removed every 4 h for volume scanning over a period of 24 h and recorded every 24 h thereafter, with the volumes recorded as V1, V2, V3, etc. The swelling endpoint occurred when the gel volume fluctuated within less than 1.0 cm^3 for 3 consecutive days. The swelling curves were plotted, and the final swelling rates were compared [25].

2.5 Experiments on the moisturizing properties of hydrogels

(1) The initial weights of the 4 hydrogels in each group were recorded, and the average value was recorded as $\overline{m}_0$. (2) The average weight at the endpoint of colloid swelling was denoted as $\overline{m}_1$. The colloid was placed in a 37 °C constant temperature box, its mass was measured every 5 h for the first 25 h, after which it was measured once a day until the mass change for the next 3 days was less than 0.5 g. The colloid was removed, and any excess water on the surface was removed before weighing, which was recorded as $\overline{m}_t$. (3) Finally, the moistening curve (the relationship between average quality and time) was drawn.

The formula for calculating the moisturizing rate R (%) is $R(\%) = [(\overline{m}_t - \overline{m}_0)/(\overline{m}_1 - \overline{m}_0) \times 100\%]$, where $\overline{m}_0$, $\overline{m}_1$ and $\overline{m}_t$ are the initial weight of the finished gel, the weight after full swelling, and the weight of the hydrogels at each time point, respectively.

2.6 Scanning electron microscopic observation of the hydrogels (SEM test)

The hydrogel was freeze-dried under vacuum, and then the sample was sliced and pasted on a conductive gel. The specimens were attached to a Lon Sputtering Apparatus (HITACHI MC1000) using carbon stickers and sputter-coated with gold for 30 s. Images were obtained with a scanning electron microscope.

2.7 Hemolysis rate experiments with hydrogels

(1) Each group of hydrogels was cut into 1 × 1 × 1 cm cubes at room temperature. (2) The samples were soaked in 75% alcohol for 5 min and then irradiated with a UV lamp for 1 h. Finally, the mixture was frozen until it was completely solid and made into a powder. (2) The powdered gel was dissolved in 5 ml of normal saline to form a suspension; 5 ml of pure normal saline was used as the negative control group, and 5 ml of pure deionized water was used as the positive control group. Each group of liquids was connected to a centrifuge tube (NEST 601001). (3) Fresh anticoagulant rabbit blood was prepared at a 1:1 dilution. (4) The above centrifuge tubes were placed in a 37 °C water bath for 20 min, and after 20 min, 200 µl of diluted fresh anticoagulant-treated rabbit blood was added. The tubes were kept warm for another half hour and centrifuged at a speed of 3000 rpm for 5 min. (5) After centrifugation, the supernatant was collected and placed on an enzyme-linked immunosorbent assay (ELISA) plate. The absorbance (OD) at 562 nm was measured using a UV spectrophotometer, and the experiment was repeated 4 times.

The formula for calculating the hemolysis rate was as follows:

$$\mathrm{HR} = (\text{OD of sample group-OD of the negative group})/(\text{OD of a positive group-OD of the negative group}) * 100\%.$$

2.8 L929 cytotoxicity assay with hydrogels

The cytotoxicity of the hydrogels on L929 cells was evaluated using a cell counting kit-8 (CCK-8) assay (Dojindo Co., Kumamoto, Japan). In the experimental group, the hydrogels were 0.5 × 0.5 × 0.5 cm in size, soaked in 75% alcohol for 5 min, and then irradiated with UV light for 1 h. According to the manufacturer's protocol, the hydrogels were placed into 96-well plates. L929 cells (5000 cells/well) were encapsulated in hydrogels, while a control group was established. After that, the 96-well plates were substantially cultured for 7 days at 37 °C. The end point of the experiment was the seventh day. A microplate reader (Leica Microsystems, Germany) was used to quantify the absorbance at a wavelength of 450 nm. All experiments were repeated three times. Cell viability= (OD value of control *group cell* − OD value of hydrogels group cell/OD value *of control group cell*) × 100%.

2.9 Animals and ethics statement

A total of 35 healthy, 8-week-old Sprague Dawley rats (male, average weight 280–300 g) from the Experimental Animal Center of Ningbo University (License No. SYXK [ZJ] 2019-0005) were individually housed in standard experimental cages in an environment-controlled room (temperature 22–25 °C, humidity 60–70%, 12-/12-h light: dark cycle), and they were provided with contaminant-free feed and drinking water. All procedures involving rats were approved by the Animal Research Committee of Ningbo University (X1701462), and the rats were cared for according to the Ethical Guidelines on Animal Experimentation of Laboratory Animals of China National Institutes of Health.

2.10 Self-expanding hydrogels in rats

Group A (27.8% CS-AM group): Five rats were subjected to hydrogel placement under the skin of the back. Group B

(27.8% CS-AM group): five rats were subjected to hydrogel placement under the skin of their necks. Group C (AM group): Five rats were subjected to hydrogel placement under the skin of their backs. Group D (AM group): Five rats were subjected to hydrogel placement under the skin of their necks. Group E (blank control group): Five rats received no treatment. (Note: The size of the hydrogel samples placed on the backs of the rats was $2 \times 3 \times 1$ cm, and the size of the hydrogel samples placed on the necks of the rats was $1 \times 2 \times 1$ cm. After suturing, erythromycin ointment was applied to the wound every day. Anesthesia consisted of 10% chloral hydrate and ether anesthetics).

2.11 Silicone dilator in rats

We customized a silicone dilator with a 10 ml capacity and placed it subcutaneously as a control. Five rats were subjected to silicone dilators placed under the skin their backs, and 5 rats were subjected to silicone dilators placed under the skin of their necks. At each observation point, water was added to the expander to a volume equal to the maximum expansion volume of the experimental group (±0.5 ml).

2.12 Hematoxylin and eosin (H&E) staining

The tissue samples around the hydrogel were fixed in 4% paraformaldehyde for 24 h and then embedded in paraffin. The embedded tissue samples were fixed on a microtome and cut into 4-μm-thick slices, which were subsequently stained with an H&E staining kit. (Solarbio Science & Technology G1120). We manually counted the number of inflammatory cells per unit area (/mm2) under an optical microscope (200x magnification, Olympus, Tokyo, Japan). The cells were counted in six random fields from three random slices of each tissue sample.

2.13 Immunohistochemistry (IHC)

Sections from each group ($n = 6$) were deparaffinized with xylene and rehydrated in a graded ethanol series. After washing, endogenous peroxidase activity was blocked with 3% H2O2, and antigen retrieval was carried out in a 10.2 mM sodium citrate buffer for 20 min at 95 °C. After blocking with 10% normal goat serum for 30 min, the sections were incubated with antibodies against IL-6 (Abcam, ab214429) overnight at 4 °C. Finally, the sections were incubated with goat anti-rabbit IgG H&L (DyLight® 594; Abcam, ab96885) and counterstained with hematoxylin. The sections were imaged at 200x magnification with a DP2-BSW image acquisition system (Olympus, Tokyo, Japan). The integral absorbance was quantified with Image-Pro Plus v6.0 software (Cybernetics, MD, USA) to compare the protein expression levels. Six random fields were counted from three random sections of each tissue sample.

2.14 Immunofluorescence staining

Sections ($n = 6$) were deparaffinized and rehydrated in a graded ethanol series and incubated in 10% normal goat serum supplemented with 0.2% Triton X-100 (Aladdin, T109027) at room temperature for 30 min. After blocking, the sections were incubated overnight with primary antibodies against CD31 (Abcam, ab28364, 1:200) and α-SMA (Abcam, ab7817, 1:200) at 4 °C, followed by incubation with tetramethylrhodamine-labeled rabbit IgG-H&L (DyLight® 488; Abcam, ab96883) and goat anti-mouse IgG H&L (DyLight® 488; Abcam, ab96871) at room temperature for 1 h. An anti-fluorescence quenching agent was added after DAPI (Thermo Scientific™ 62248) staining for 2 min. All images were evaluated under a Nikon ECLIPSE Ti microscope (Nikon, Japan). Six random fields were used from three random sections of each tissue sample.

2.15 Statistical analyses

All the data are expressed as the mean ± standard deviation (SD). Statistical analysis was performed using SPSS software version 22.0 (IBM Corp., Armonk, NY, USA) with independent-sample t tests. $P < 0.05$ indicated statistical significance.

3 Results

3.1 Macro appearance of the self-expanding hydrogel morphology

Figure 3A shows the morphological changes of the 27.8% CS-AM self-expanding hydrogels during in vitro swelling experiments, with Days 1, 7, and 14 of swelling selected as examples. Figure 3B shows the morphological changes in the 27.8% CS-AM hydrogel after complete swelling in a 37 °C incubator for the holding tests, with water loss occurring on Days 1, 7, and 14, and water loss occurring on Day 14. Figure 3C shows that the visible gel changes from a transparent liquid to a white solid due to heating; Fig. 3D shows the preliminary viscosity of the gel. If the contact surface is dry, the viscosity of the gel is obvious when it is grasped with the naked hand. If the wet gel on the contact surface is not sticky, it cannot adhere to the skin. Figure 3E shows a simple extension and pull test of the hydrogel, which was lifted with tweezers and stretched by hand.

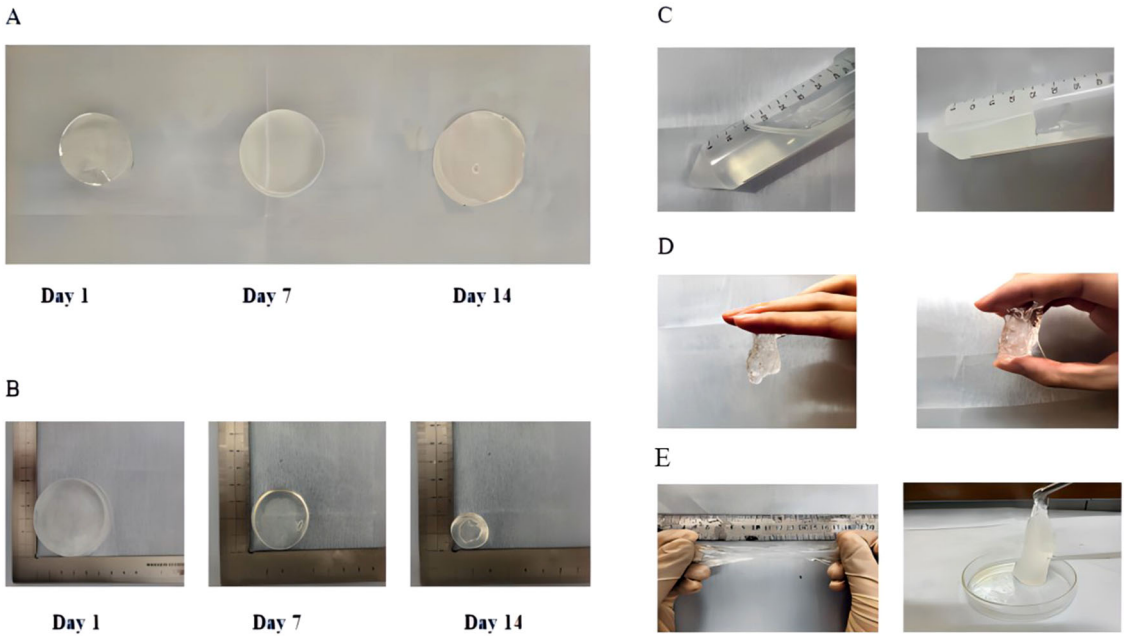

Fig. 3 Macro appearance of the self-expanding hydrogel morphology. **A\B** Morphological changes in the CS-AM self-expanding hydrogels during in vitro swelling and in vitro moisturization; **C** Gel molding '**D** Viscosity of gel. **E** Simple extension and pull test of the hydrogel

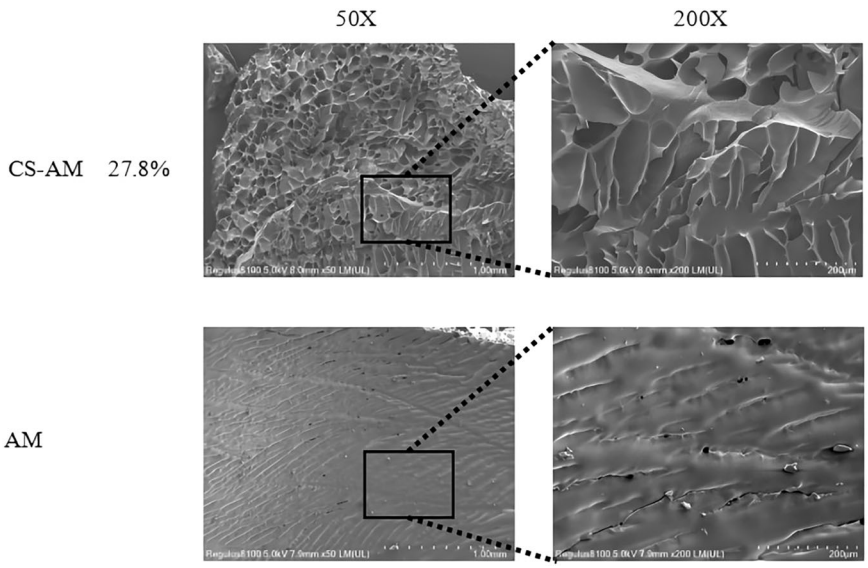

Fig. 4 Scanning electron micrographs of the pore architecture of the self-expanding hydrogel

3.1.1 Electron microscopy of a self-expanding hydrogel

Scanning electron microscopy images of the morphology of the 27.8% CS-AM self-expanding hydrogels in Group A and the morphology of the AM self-expanding hydrogels in Group B were obtained. Figure 4 shows that the CS-AM group hydrogels have a porous, three-dimensional structure and are spatially cross-distributed, while the AM hydrogels have a single morphology and a scattered and unstable structure.

3.2 Swelling curves of self-expanding hydrogels

The 13.9%, 27.8%, and 55.6% groups maintained the same volume after complete swelling. The 41.1% CS-AM group reached the maximum swelling rate. However, the 41.7% and 0% groups showed expansion fragmentation after complete swelling, thus showing a decreasing trend in terms of volume (Fig. 5). Therefore, 27.8% CS-AM has the best overall performance and is the optimal choice.

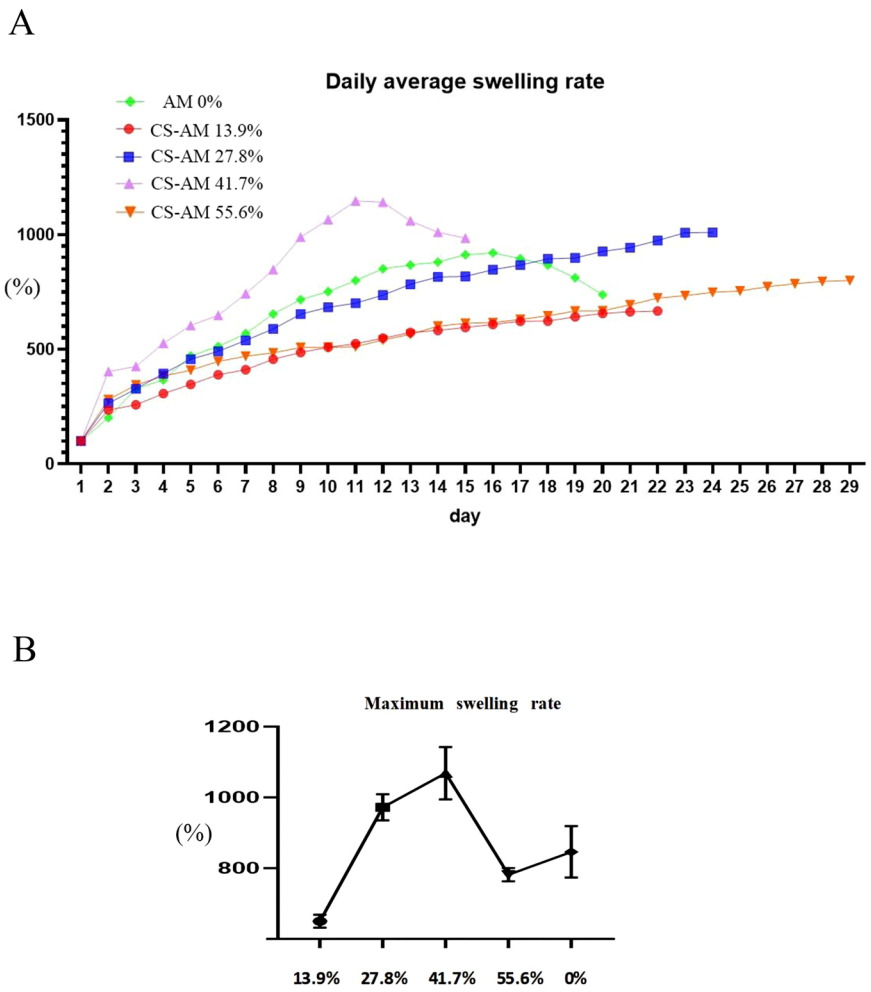

Fig. 5 **A** Expansion curves for the five groups of CS-AM self-swelling hydrogels: 0% (pure AM group), 13.9%, 27.8%, 41.7%, and 55.6%. **B** Maximum swelling rates of the five groups of CS-AM self-swelling hydrogels: 0% (pure AM group), 13.9%, 27.8%, 41.7%, and 55.6%

3.3 Tensile and compression testing of self-expanding hydrogels

The elongation of the gel in the 27.8% CS-AM group reached a maximum of 900 ± 20%, while the elongation of the gel in the AM group reached a maximum of 765 ± 10%. The elongation of the CS-AM group was significantly different from that of the AM group ($P < 0.05$), indicating that the addition of CS improved the ductility of the AM hydrogel (Fig. 6 and Table 1).

The hydrogels in the AM group, CS-AM 13.9% group, and CS-AM 41.7% group reached 100% compression (due to both the pressure plateau and pressure application surface contact), and the gel did not break. In contrast, the hydrogels of the CS-AM 27.8% and CS-AM 55.6% groups broke when the maximum pressure was reached, and the CS-AM 27.8% group was able to withstand a maximum pressure of 660 kPa. The maximum pressure in the CS-AM group was greater than that in the AM group ($P < 0.05$), indicating that the addition of CS enhanced the structural stability of the AM hydrogel (Fig. 6 and Table 1).

3.4 Testing the moisture retention properties of self-expanding hydrogels

The self-expanding hydrogels in the 0% AM group and the 41.7% CS-AM group were excluded from this moisture test because the gels of these groups broke down when the maximum swelling state was met and their normal forms could not be maintained. The 27.8% group in the graph lost water slowly overall at approximately 4.9 g/day and reached a stable state earlier, while the 13.9% group lost water the fastest at approximately 5.4 g/day (Fig. 7). The difference in moisturizing time among the groups was not significant ($P > 0.05$), indicating that there was no significant difference in moisturizing performance among the groups.

3.5 Toxicity testing of self-expanding hydrogels

The hemolysis rate tended to decrease when the proportion of chitosan in the self-swelling hydrogel component increased, with the AM group showing the highest rate of hemolysis at approximately 17.2%, while the CS-AM 55.6% group reached the lowest value at approximately

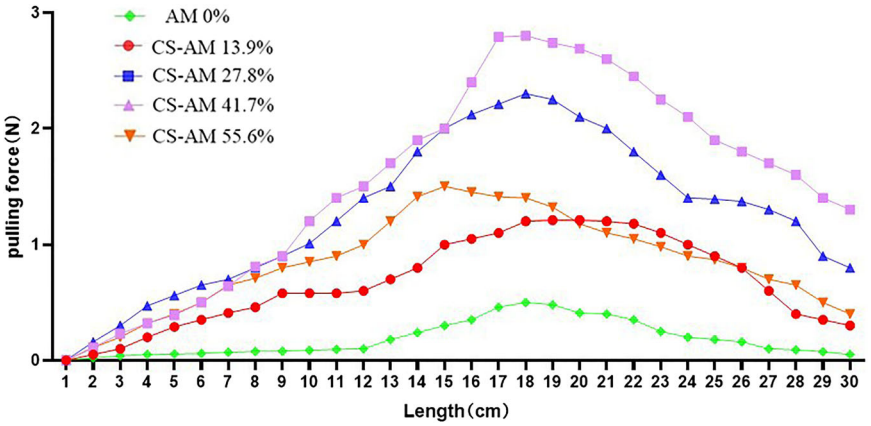

Fig. 6 Tensile test curve of the self-expanding hydrogel

Table 1 Elongation of each group of colloids when the maximum tensile force is reached

	group	L0 (cm)	L1 (cm)	Elongation (%)
CS-AM	13.9%	2.0 ± 0.1	16.5 ± 0.3	825 ± 15%
	27.8%	2.0 ± 0.1	18.0 ± 0.4	900 ± 20%
	41.7%	2.0 ± 0.1	17.1 ± 0.3	855 ± 15%
	55.6%	2.0 ± 0.1	16.8 ± 0.3	840 ± 15%
AM	0%	2.0 ± 0.1	15.3 ± 0.2	765 ± 10%

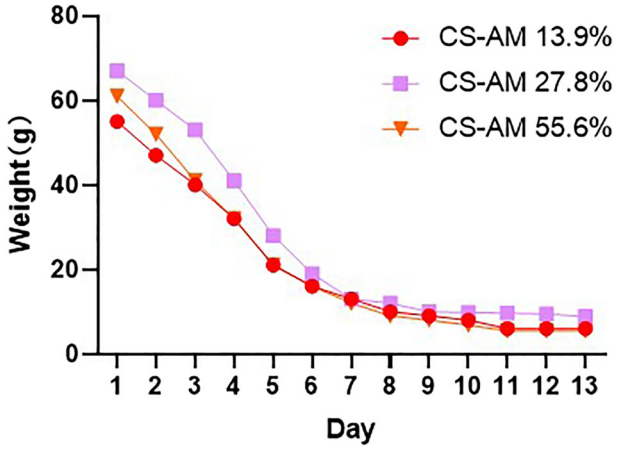

Fig. 7 Moisture retention performance curves of three groups of self-expanding CS-AM hydrogels (13.9%, 27.8%, and 55.6%)

1.8% (Fig. 8). The cytotoxicity study was carried out using the CCK8 method to measure the biocompatibility of the hydrogel. The inactivation rate of L929 fibroblasts was analyzed in the form of a statistical chart, with the end of the seventh day as the experimental endpoint. The inhibitory effect of the hydrogel on L929 (mouse embryonic fibroblast) cells was also influenced by the percentage of CS, and this effect followed the same trend as that shown by the hemolysis rate, with the rate of inhibition of cell activity decreasing as the mass fraction of CS increased, reaching a minimum of 11.3% in the CS-AM group, while the rate of inhibition was greater than 50% in the AM group (Fig. 9). The hemolysis rate of the CS-AM group was compared with that of the AM group ($P < 0.05$), indicating that the addition of CS improved the material toxicity of the AM hydrogel.

3.6 In vivo experiments with self-expanding hydrogels

In the aforementioned in vitro tests, the 27.8% CS-AM group of self-expanding hydrogels had stable mechanical strength, low biological toxicity, good swelling, and good moisturizing properties, so we selected this group of hydrogels for subcutaneous experiments in rats and prepared silicone dilators as a control (Fig. 10).

3.7 Expression curve of the skin area during the subcutaneous expansion of the self-expanding hydrogel in rats

The extent of hydrogel expansion in the neck region was significantly lower in the AM and CS-AM groups than in the control group. Due to the absorption of the hydrogel, the skin expansion area of the AM group decreased. In addition, the expansion effect of the AM group on the back and neck was significantly lower than that of the CS-AM group, and the difference was significant. The time for complete subcutaneous expansion in the CS-AM group was slightly longer than that in the AM group, and the difference in expansion time was not significant (Fig. 11A and B).

3.8 Pathological examination of soft tissue around self-expanding hydrogels

The infiltration level of inflammatory cells in each group was analyzed through HE staining. Compared to those in the CS-AM group, the hydrogels in the AM group were more likely to cause inflammatory changes in the

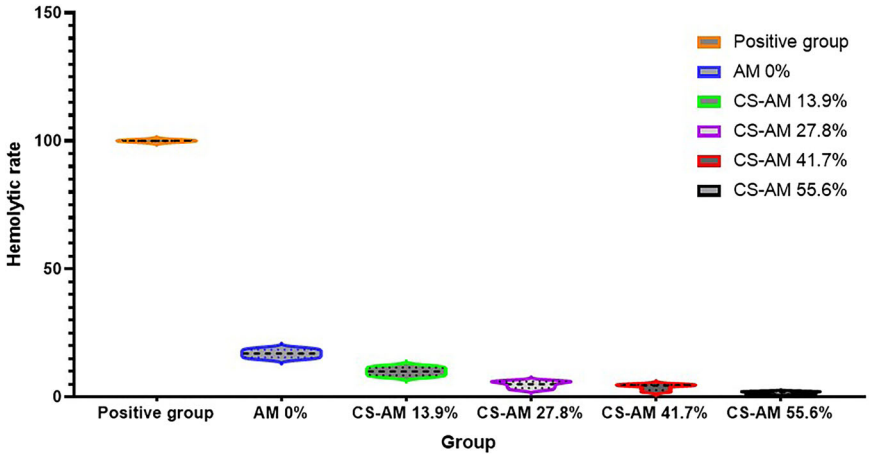

Fig. 8 Range of hemolysis rates for each group of hydrogels

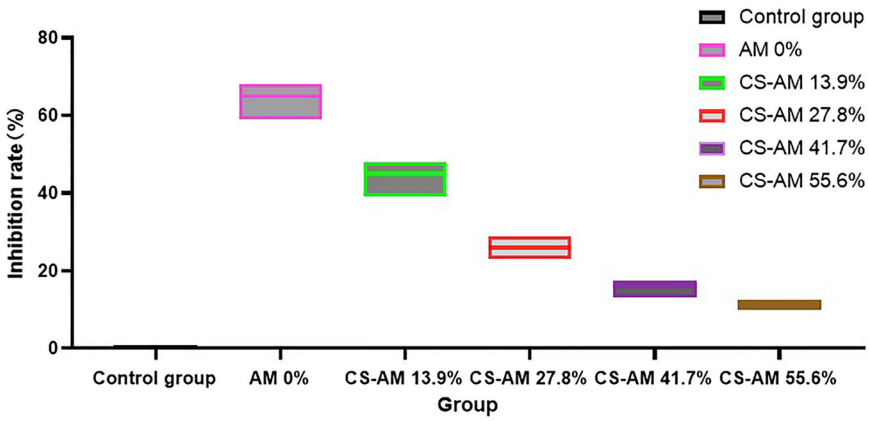

Fig. 9 L929 cell cytotoxicity assays of self-expanding hydrogels

surrounding tissue (Fig. 12A). IL-6 expression was detected by IHC to assess inflammatory infiltration in each group. As shown in Fig. 12B, inflammation and infection were most likely to occur in the AM group, while the CS-AM 27.8% group exhibited the lowest inflammation and infection rates. However, compared to the blank control group, this group still exhibited significant skin and soft tissue inflammation. This inflammation was found to be significant by measuring the integral absorbance of IL-6. When hydrogels and silica gel expanders were used for skin expansion, subcutaneous inflammation occurred, and the inflammatory effect in the pure AM group became more prominent. This finding is related to the autotoxicity of the pure AM group. Compared with the CS-AM 27.8% group, the addition of CS had a significant detoxification effect on the hydrogel. Immunofluorescence staining for CD31 and α-SMA was performed to assess angiogenesis in each group. We labeled the vasculature with CD31 (red) and α-SMA (green), and the nuclei in the dermis of the tissue were labeled with DAPI (blue) (Fig. 12C). The vascular density statistics indicated that the placement of the hydrogel caused compensatory proliferation of epidermal microvessels, and this proliferation was significant in the AM and CS-AM groups compared to that in the control group ($n = 6$, $p < 0.05$); however, when the AM group was compared to the CS-AM group ($p > 0.05$), there was no significant difference in vascular proliferation.

4 Discussion

With the research on hydrogel materials, permeable dilator development has been rapid [26]. Hydrogels have received much attention and are used in many fields because of their superior characteristics when compared to traditional absorbents [27]. However, these hydrogels generally have the following problems: (1) the swelling efficiency of the gel after water absorption is often difficult to control: the swelling efficiency of hydrogel implantation is highest in the first week, and rapid swelling of the gel can lead to problems such as insufficient blood flow to the skin tissue in the expansion area, and most of the materials reach swelling equilibrium within 2 weeks. (2) The final swelling volume is insufficient (the swelling equilibrium of the hydrogel). (3) Few biosafety studies [9, 28]. In recent years, the use of materials such as silicone resin or semipermeable

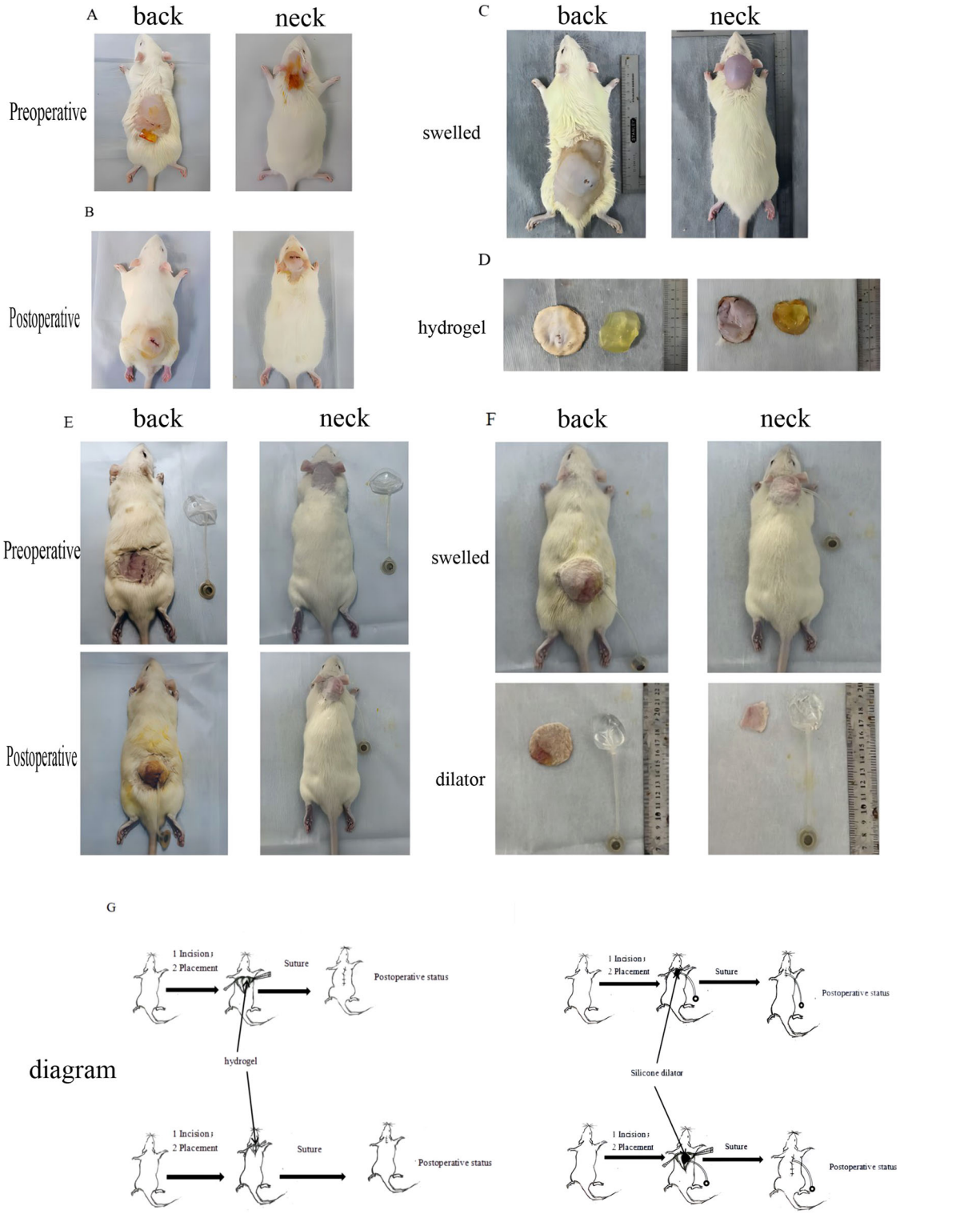

Fig. 10 Group A shows the completed skin preparation before the self-expanding hydrogel was implanted subcutaneously in the backs and necks of the rats; Group B shows the state after the hydrogel was implanted; Groups C and D show the state after the hydrogel was completely swelled under the skin of the rats; and Groups E and F show the expansion effect of the silicone dilator. Group G is a simple diagram of an animal experiment

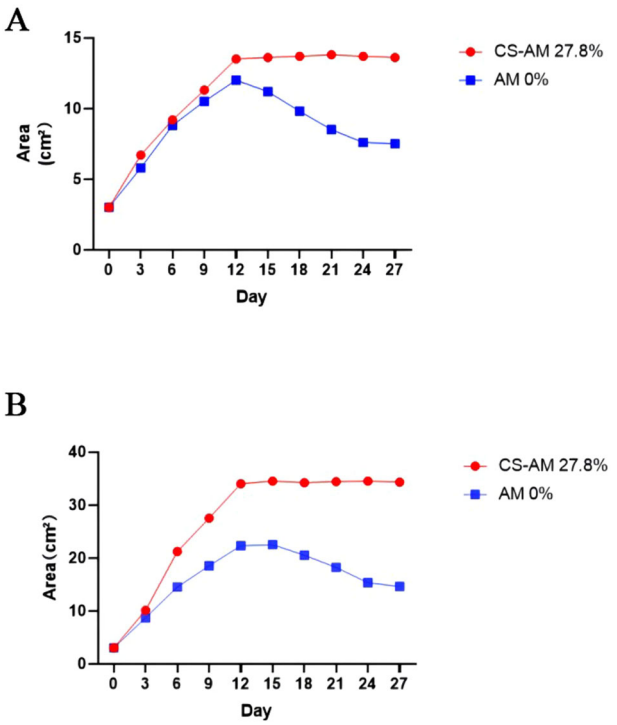

Fig. 11 Skin expansion curve of the self-expanding hydrogel during subcutaneous swelling in rats: (**A**) is the expansion of the skin on the neck, (**B**) is the expansion of the skin on the back

membranes wrapped around hydrogels to regulate the expansion rate has been proposed, but the specific effect still needs further study [29, 30].

Polyacrylamide-based hydrogels have long been used in biological and medical fields [31, 32]. Many studies have shown that polyacrylamide hydrogels can be used as an expansion body for injectable breast augmentation and soft tissue filling [33, 34]. In addition, polyacrylamide hydrogels are used as trauma adjuvants to repair wounds [21]. However, the poor mechanical properties of AM hydrogels have limited their further development [35]. Chitosan is one of the most widely used materials for the manufacture of hydrogels and is considered for use in a variety of materials because of its excellent biocompatibility, low toxicity, and immunostimulatory activity [36]. The self-expanding hydrogels obtained by incorporating acrylamide into chitosan hydrogels significantly improved the mechanical properties of the hydrogels. This result was the same as that obtained for the double network hydrogel prepared by the interpenetration of a flexible and rigid network [37, 38]. Natural macromolecular chitosan successfully enhances the mechanical properties of hydrogels, resulting in little tearing or peeling during daily activities [39]. Polymerization of a concentrated aqueous solution of acrylamide in the presence of chitosan without any chemical cross-linker produces thermoplastic and remoldable hybrid supramolecular polymeric hydrogels with high strength, stretchability, and fracture energy. The dynamic dissociation and re-association of the hydrogen bonding cross-links between the polyacrylamide and chitosan chains endows these gels with self-healing, rapid self-recovery, and excellent anti-fatigue properties [40]. In this study, we used various tests to evaluate the performance of these self-expanding chitosan-acrylamide hydrogels. The results of tensile tests suggest that the CS-AM 27.8% group of self-expanding hydrogels can extend up to 9 times their size before expansion under stress, while the elongation of the CS-AM 41.7% group decreases significantly; this is due to the excessive addition of CS molecules, which reduces the material compatibility of the structural molecules within the colloid, thereby reducing the structural strength. However, compared to that of the pure AM group in the control group, the structural enhancement caused by CS was obvious. The pressure-bearing properties of the hydrogels in each group were consistent with the tensile test results, in which for the problem of breakage under pressure in the CS-AM 27.8% and CS-AM 55.6% groups, we believe that the former has the highest mechanical strength and can withstand the highest pressure, but the cross-linked structure will be directly destroyed when the pressure-bearing threshold (660 kPa) is broken. The fracture in the CS-AM 55.6% group may be due to the excessive addition of CS, which increases the possibility of forming chitosan polymers under electrostatic action. Because the polymer has poor compatibility with CS-AM colloids, the colloidal structure is disordered and easily broken. The swelling of all hydrogel groups reached the level of expansion between the subrapid and rapid phases. The 0% group with only AM and the 41.7% CS-AM group showed expansion and breakage during the late stage of swelling. We believe that due to the absorption of water molecules into the gap of the gel structure, the structural stability is impacted and the interaction force between molecular chains is confronted and will cause damage when the maximum value is reached [41]. As an important property of hydrogels, we investigated the moisturizing ability of self-expanding hydrogels. Moisture retention performance and swelling tests were conducted to evaluate the "water storage" abilities of the self-expanding hydrogels, and scanning electron microscopy revealed that the CS-AM group hydrogels had more interlocking water channels than did the AM group hydrogels under the same field of view, and the former had an obvious three-dimensional porous structure, which proved that the CS-AM group hydrogels had more space to carry water molecules and had sufficient storage conditions. AM group hydrogels have more space to carry water molecules and sufficient storage conditions. In the moisture retention test, the 27.8% group had the slowest water loss rate and the best moisture retention performance. The results of testing material toxicity suggest that the toxicity

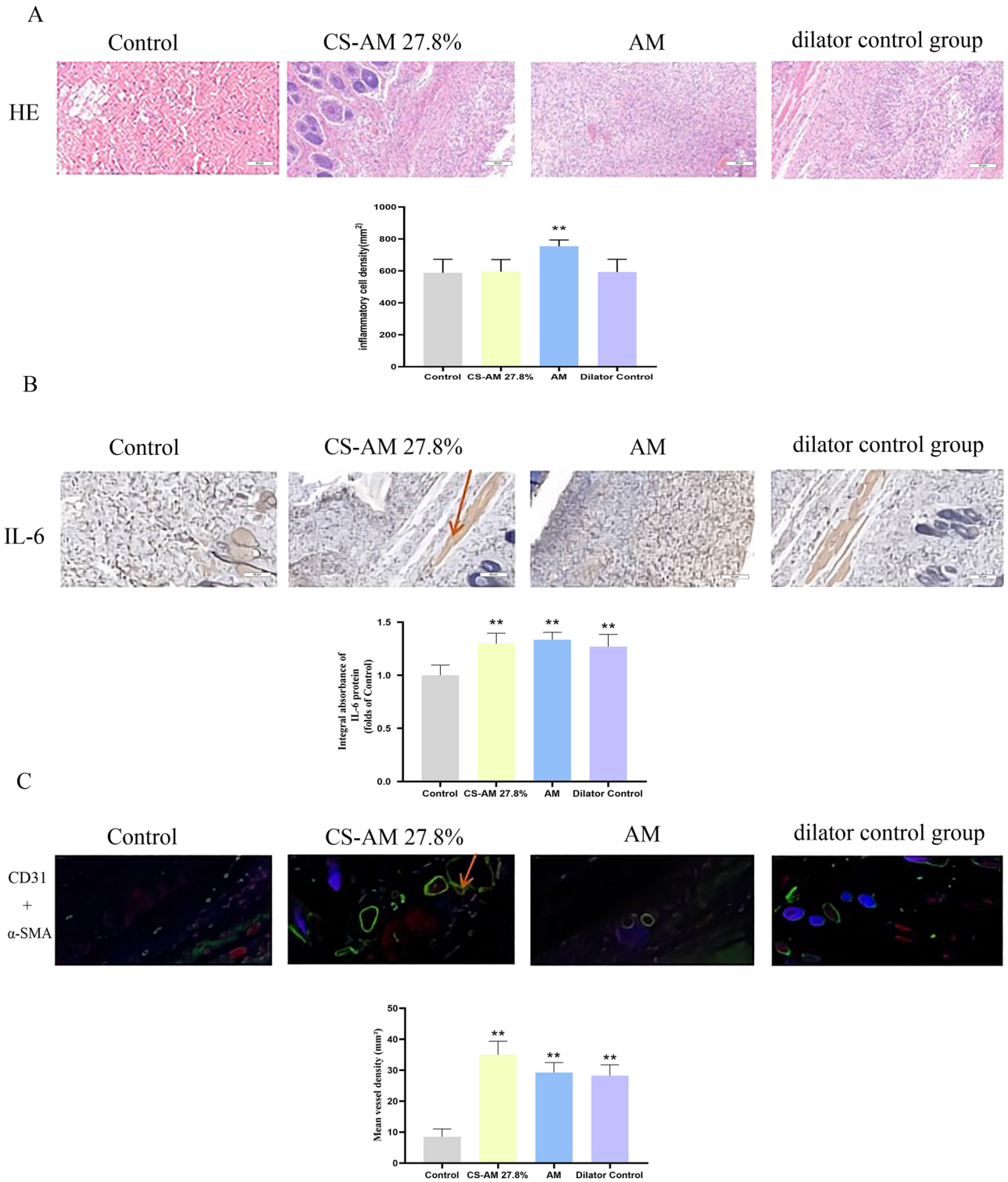

Fig. 12 **A** H&E staining showing the number of inflammatory cells in each group (original magnification, 200×; scale, 50 μm). The inflammatory cell density in each group was quantified, analyzed, and plotted as a histogram (/mm2). **B** IHC for IL-6 expression in rat connective tissue (original magnification, 200×; scale, 50 μm). The optical density values of IL-6 were quantified and analyzed. **C** Immunofluorescence for CD31 (red) and α-SMA (green) showed the blood vessels of each group (original magnification 200×; scale bar, 50 μm). The mean vessel density (MVD) in each group was quantified and analyzed, and the histogram shows the MVD in the flap (/mm2)

of the CS-AM hydrogel depends on the percentage of CS, and the greater the percentage of CS is, the lower the colloidal toxicity. Some studies have confirmed that the standard hemolysis rate of medical materials is 5%, and when the hemolysis rate of the material is greater than 5%, it is likely to cause hemolytic disease; meanwhile, when the hemolysis rate is less than 5%, the hemolytic effect is dramatically reduced, and the material can be used as an implantable medical material [42, 43]. In our study, when the proportion of chitosan in the self-expanding hydrogel component increased, the hemolysis rate tended to decrease, and all of the rates were lower than 5%. The AM group had the highest hemolysis rate, i.e., approximately 17.2%, while the CS-AM 55.6% group had the lowest value, approximately 1.8%. Moreover, from the viewpoint of the L929 cell survival rate, the addition of CS increased the cell survival rate to more than 50%. The toxicity of this material can be further reduced by adjusting the ratio of CS to AM and enhancing the reduction in toxicity during the colloid preparation process.

In this animal experiment, the skin area of the 27.8% CS-PAM hydrogel group could expand 4.0–4.5 times when the neck skin was expanded and 4.5–5.0 times when the back skin was expanded. In addition, the expansion time can be controlled between 2 and 4 weeks. This expansion effect basically meets the needs of skin and soft tissue defect clinical repair. However, pure AM undergoes deformation and fragmentation in the later stages of expansion, leading to the expansion of the skin and its subsequent retraction. Therefore, its effectiveness as a dilator is not satisfactory. The different expansion effects of hydrogels in the tight area (neck) and the loose area (back) of the skin can be used as important references for the modification of gels. In clinical cases of skin defects, expansion is not always performed in relaxed skin areas Therefore, the expansion performance of the hydrogel can be improved to meet this demand so that a hydrogel expander matching the skin area tightness can be prepared.

We analyzed the pathological findings of the surrounding tissues in the expansion area and concluded that the early placement of the self-expanding hydrogel produced local edema after compression of the surrounding tissues. However, the edema resolved substantially after the compensatory proliferation of microvessels in the middle stage, causing only a transient disturbance of the microcirculation [44], and the proliferation of microvessels could be used as an indicator of skin survival [45, 46]. Recent studies have shown that substrate elasticity and topographical guidance are crucial factors for regulating tissue regeneration [47]. Interestingly, our research also revealed that polyacrylamide/chitosan (AM/CS) composite hydrogels can promote angiogenesis. Inflammatory indicators were detected in both the CS-AM and AM groups, and their presence may be related to prolonged foreign body irritation; however, there was no extensive cellular necrosis, a result similar to local inflammation caused by other skin expanders [48, 49]. The AM group showed more extensive inflammatory changes, which is consistent with the results of previous in vitro material toxicity tests.

In animal experiments, the dilator group exhibited a significant expansion effect. Compared with the experimental group of hydrogels, the former requires multiple injections of water, which may increase the risk of infection. In addition, some silicon capsules were exposed in the rat experiment. The inflammatory pathological results showed that there was no significant difference between the dilator group and the 27.8% CS-AM group, but in terms of promoting angiogenesis, angiogenesis in the dilator group was significantly lower than that in the 27.8% CS-AM group, which indicated that the hydrogel also promoted wound healing. However, this study of the self-expanding hydrogel-type expander still has some limitations, such as incomplete descriptions of colloidal ductility and viscosity. In the future, we will still work to address the shortcomings of this material and provide convincing evidence by conducting large animal experiments with standard animal models and detailed data analysis to apply it in clinical applications.

Funding The author(s) declare that financial support was received for the research, authorship, and/or publication of this article. This work was supported by grants from Municipal Key R&D Program of Ningbo (2022Z146), Ningbo Top Medical and Health Research Program (No.2022020506).

Compliance with ethical standards

Conflict of interest The authors declare no competing interests.

References

1. Zhang C, Shao Z, Chen Z, Lin C, Hu S, Lou Z, et al. Hydroxysafflor yellow A promotes multiterritory perforating flap survival: an experimental study.[J]. Am J Transl Res. 2020;12:4781–94.

2. Chen Z, Wu H, Yang J, Li B, Ding J, Cheng S. et al. Activating Parkin-dependent mitophagy alleviates oxidative stress, apoptosis, and promotes random-pattern skin flaps survival[J]. Commun Biol. 2022;5:616. https://doi.org/10.1038/s42003-022-03556-w.
3. Neumann CG. The expansion of an area of skin by progressive distention of a subcutaneous balloon; use of the method for securing skin for subtotal reconstruction of the ear.[J]. Plast Reconstr Surg. 1957;19:124–30. https://doi.org/10.1097/00006534-195702000-00004.
4. Guo Y, Song Y, Xiong S, Wang T, Liu W, Yu Z, et al. Mechanical stretch induced skin regeneration: molecular and cellular mechanism in skin soft tissue expansion.[J]. Int J Mol Sci. 2022;23. https://doi.org/10.3390/ijms23179622.
5. Al Madani JO. Second generation self-inflating tissue expanders: a two-year experience. Plast Surg Int. 2014;2014:457205. https://doi.org/10.1155/2014/457205.
6. Wang Y, Qi H. Perfect combination of the expanded flap and 3D printing technology in reconstructing a child's craniofacial region[J]. Head Face Med. 2020;16. https://doi.org/10.1186/s13005-020-00219-1.
7. Al-Harganee A, Enescu DM. Tissue expansion: Principles, techniques & unwanted results[J]. Arch Balk Med Union. 2015;50:620–3.
8. Swan MC, Bucknall DG, Goodacre TE, Czernuszka JT. Synthesis and properties of a novel anisotropic self-inflating hydrogel tissue expander[J]. Acta Biomater. 2011;7:1126–32. https://doi.org/10.1016/j.actbio.2010.10.017.
9. Hrib J, Chylikova Krumbholcova E, Duskova-Smrckova M, Hobzova R, Sirc J, Hruby M. et al. Hydrogel tissue expanders for stomatology. Part II. Poly(styrene-maleic anhydride) Hydrogels[J]. Polymers. 2019;11:1087. https://doi.org/10.3390/polym11071087.
10. Arain AR, Cole K, Sullivan C, Banerjee S, Kazley J, Uhl RL. Tissue expanders with a focus on extremity reconstruction.[J]. Expert Rev Med Devices. 2018;15:145–55. https://doi.org/10.1080/17434440.2018.1426457.
11. Gronovich Y, Binenboym R, Retchkiman M, Eizenman N, Lotan A, Stuchiner B, et al. Reconstruction in plastic surgery using osmotic tissue expanders[J]. Harefuah 2015;154:155–8, 213.
12. Chang Y, Zhang F, Liu F, Shi L, Zhang L, Zhu H, et al. Self-swelling tissue expander for soft tissue reconstruction in the craniofacial region: An in vitro and in vivo evaluation[J]. Bio Med Mater Eng. 2021:1–14. https://doi.org/10.3233/BME-211224.
13. Chang M, Liu X, Meng L, Wang X, Ren J. Xylan-based hydrogels as a potential carrier for drug delivery: effect of pore-forming agents.[J]. Pharmaceutics. 2018. https://doi.org/10.3390/pharmaceutics10040261.
14. Yue Y, Wang X, Wu Q, Han J, Jiang J. Assembly of polyacrylamide-sodium alginate-based organic-inorganic hydrogel with mechanical and adsorption properties[J].Polymers. 2019;11. https://doi.org/10.3390/polym11081239.
15. Călina I, Demeter M, Scărișoreanu A, Sătulu V, Mitu B. One step e-Beam radiation cross-linking of quaternary hydrogels dressings based on chitosan-Poly(Vinyl-Pyrrolidone)-Poly(Ethylene Glycol)-Poly(Acrylic Acid). Int J Mol Sci. 2020;21:9236. https://doi.org/10.3390/ijms21239236.
16. Getachew BA, Kim SR, Kim JH. Self-healing hydrogel pore-filled water filtration membranes. Environ Sci Technol. 2017;51:905–13. https://doi.org/10.1021/acs.est.6b04574.
17. Ku M, Cheung S, Slattery W, Pierstorff E. An extended release ciprofloxacin/dexamethasone hydrogel for otitis media[J]. Int J Pediatr Otorhinolaryngol. 2020;138:110311. https://doi.org/10.1016/j.ijporl.2020.110311.
18. Wang Z, Lin M, Wang M, Song X, Zhang C, Dong Z. et al. Polymerizable microsphere-induced high mechanical strength of hydrogel composed of acrylamide[J]. Materials. 2018;11:880. https://doi.org/10.3390/ma11060880.
19. Liao WC, Lilienthal S, Kahn JS, Riutin M, Sohn YS, Nechushtai R. et al. pH- and ligand-induced release of loads from DNA-acrylamide hydrogel microcapsules.[J]. Chem Sci. 2017. https://doi.org/10.1039/c6sc04770j.
20. Wang W, Meng Q, Li Q, Liu J, Zhou M, Jin Z, et al. Chitosan derivatives and their application in biomedicine. Int J Mol Sci. 2020;21:487. https://doi.org/10.3390/ijms21020487.
21. Lu B, Han X, Zou D, Luo X, Liu L, Wang J. et al. Catechol-chitosan/polyacrylamide hydrogel wound dressing for regulating local inflammation.[J]. Mater Today Bio. 2022;16:100392. https://doi.org/10.1016/j.mtbio.2022.100392.
22. Ahmadi FZ, Oveisi SM, Amoozgar SZ. Chitosan based hydrogels: characteristics and pharmaceutical applications.[J]. Res Pharm Sci. 2015;10:1–16.
23. Rashki S, Asgarpour K, Tarrahimofrad H, Hashemipour M, Ebrahimi MS, Fathizadeh H, et al. Chitosan-based nanoparticles against bacterial infections. Carbohydr Polym. 2021;251:117108. https://doi.org/10.1016/j.carbpol.2020.117108.
24. Aavik A, Kibur RT, Lieberg J, Lepner U, Aunapuu M, Arend A. Cold-stored venous allografts in different preserving solutions: a study on changes In Vein Wall morphology[J]. Scand J Surg. 2018. https://doi.org/10.1177/1457496918783728.
25. Yang L. Nano-hydrogel for the treatment of depression and epilepsy.[J]. J Biomed Nanotechnol. 2022;18:1097–105. https://doi.org/10.1166/jbn.2022.3318.
26. Hollins A, Mundy LR, Atia A, Levites H, Peterson A, Erdmann D. Tissue expander scrotal reconstruction.[J]. Plast Reconstr Surg Glob Open. 2020;8:e2714. https://doi.org/10.1097/GOX.0000000000002714.
27. Ibrahim AGJAJoPS, Technology. Synthesis of Poly(Acrylamide-Graft-Chitosan) hydrogel: optimization of the grafting parameters and swelling studies. 2019;5:55–62. https://doi.org/10.11648/j.ajpst.20190502.13.
28. Hou Z, Xian J, Chang Q, Wei W, Li D. Digital evaluation of orbital development after self-inflating hydrogel expansion in Chinese children with congenital microphthalmia[J]. J Plastic Reconstr Aesthet Surg. 2016. https://doi.org/10.1016/j.bjps.2016.01.011.
29. Obdeijn MC, Nicolai J, Werker P. The osmotic tissue expander: a three-year clinical experience. J Plast Reconstr Aesthet Surg. 2009;62:1219–22. https://doi.org/10.1016/j.bjps.2007.12.088.
30. Anwander T, Schneider M, Gloger W, Reich RH, Appel T, Martini M, et al. Investigation of the expansion properties of osmotic expanders with and without silicone shell in animals.[J]. Plast Reconstr Surg. 2007;120:590–5. https://doi.org/10.1097/01.prs.0000270297.58498.18.
31. Park J, Kim M, Choi S, Sun JY. Self-healable soft shield for γ-ray radiation based on polyacrylamide hydrogel composites[J]. Sci Rep. 2020;10. https://doi.org/10.1038/s41598-020-78663-x.
32. Syla N, Aliaj F. Swelling and mechanical properties of polyacrylamide based hydrogels prepared by radiation induced polymerization. J Eng Appl Sci. 2018;13:7205–9. https://doi.org/10.3923/jeasci.2018.7205.7209.
33. Qian B, Xiong L, Guo K, Wang R, Yang J, Wang Z. et al. Comprehensive management of breast augmentation with polyacrylamide hydrogel injection based on 15 years of experience: a report on 325 cases. Ann Transl Med. 2020;8:475. https://doi.org/10.21037/atm.2020.03.68.
34. Cheng NX, Liu LG, Hui L, Chen YL, Xu SL. Breast cancer following augmentation mammaplasty with polyacrylamide hydrogel (PAAG) injection. Aesthet Plast Surg. 2009;33:563–9. https://doi.org/10.1007/s00266-008-9298-4.
35. Zhou C, Wu Q. A novel polyacrylamide nanocomposite hydrogel reinforced with natural chitosan nanofibers.[J]. Colloids Surf B Biointerfaces. 2011;84:0–62. https://doi.org/10.1016/j.colsurfb.2010.12.030.

36. Lan YT, Cheng QP, Xu J, Lin SH, Lin JM, Hsu SH. Gelation and the self-healing behavior of the chitosan-catechol hydrogel. Polymers (Basel). 2022;14:4614. https://doi.org/10.3390/polym14214614.
37. Jing Z, Xu A, Liang YQ, Zhang Z, Yu C, Hong P, et al. Biodegradable Poly(acrylic acid-co-acrylamide)/Poly(vinyl alcohol) double network hydrogels with tunable mechanics and high self-healing performance. Polymers (Basel). 2019;11. Published online 2019/06/05. https://doi.org/10.3390/polym11060952.
38. Xu X, Jerca VV, Hoogenboom R. Bioinspired double network hydrogels: from covalent double network hydrogels via hybrid double network hydrogels to physical double network hydrogels. Mater Horiz. 2021;8:1173–88. https://doi.org/10.1039/d0mh01514h.
39. Kamoun EA, Kenawy ES, Chen X. A review on polymeric hydrogel membranes for wound dressing applications: PVA-based hydrogel dressings. J Adv Res. 2017;8:217–33. https://doi.org/10.1016/j.jare.2017.01.005.
40. Dutta A, Maity S, Das RK A. Highly stretchable, tough, self-healing, and thermoprocessable polyacrylamide–chitosan supramolecular hydrogel[J]. Macromol Mater Eng. 2018;303. https://doi.org/10.1002/mame.201800322.
41. Panyamao P, Ruksiriwanich W, Sirisa-Ard P, Charumanee S. Injectable thermosensitive chitosan/pullulan-based hydrogels with improved mechanical properties and swelling capacity. Polymers (Basel). 2020;12:2514 https://doi.org/10.3390/polym12112514.
42. Jiang H, Wang XB, Li CY, Li JS, Xu FJ, Mao C. et al. Improvement of hemocompatibility of polycaprolactone film surfaces with zwitterionic polymer brushes[J]. Langmuir. 2011;27:11575–81. https://doi.org/10.1021/la202101q.
43. Maamouri S, Zitouni K, Zairi I. Complications of head and neck expansion: Acting on modifiable factors. A study of 98 prothesis.[J]. Ann Chir Plast Esthet. 2021;66:385–94. https://doi.org/10.1016/j.anplas.2021.06.004.
44. Kaner D, Zhao H, Terheyden H, Friedmann A. Submucosal implantation of soft tissue expanders does not affect microcirculation[J]. Clin Oral Implants Res. 2014;25:867–70. https://doi.org/10.1111/clr.12158.
45. Chen Z, Zhang C, Ma H, Huang Z, Li J, Lou J, et al. Detrimental effect of sitagliptin induced autophagy on multiterritory perforator flap survival. Front Pharmacol. 2020;11:951. https://doi.org/10.3389/fphar.2020.00951.
46. Wu H, Zhang C, Chen Z, Lou J, Ding J, Wang L, et al. Distal arterialized venous supercharging improves perfusion and survival in an extended dorsal three-perforasome perforator flap rat model. Plast Reconstr Surg. 2021;147:957e–966e. https://doi.org/10.1097/prs.0000000000007990.
47. Liu F, Xu J, Liu A, Wu L, Wang D, Han Q. et al. Development of a polyacrylamide/chitosan composite hydrogel conduit containing synergistic cues of elasticity and topographies for promoting peripheral nerve regeneration[J]. Biomater Sci. 2022;10:4915–32. https://doi.org/10.1039/d2bm00327a.
48. Omranifard M, Heidari M, Farajzadegan Z. The volume of fluid injected into the tissue expander and the tissue expansion. J Res Med Sci. 2014;19:1163–6.
49. Johnson A, Kong F, Miao S, Lin HV, Thomas S, Huang YC, et al. Therapeutic effects of antibiotics loaded cellulose nanofiber and κ-carrageenan oligosaccharide composite hydrogels for periodontitis treatment. Sci Rep. 2020;10:18037. https://doi.org/10.1038/s41598-020-74845-9.